standard deviation values. From these diameter values, these particles are expected to be the secondary associates of the polymeric micelles. However, further morphological analyses are required for characterization of these micelle structures in the future study.

3.3. T_1 measurement

A function as a contrast agent was evaluated according to the function's ability to shorten the T_1 longitudinal relaxation time of protons of water. The T_1 water proton relaxation time of both the PEG-P(Asp(DTPA-Gd)) and the prepared micelle solutions was measured through ^{1}H-NMR (400 MHz) at three concentrations ([Gd]=0.059–1.5 mM) at 23 °C in a mixture of 20% D_2O and 80% H_2O. Then, relaxivity R_1 was calculated from the formula described in Materials and methods.

The relaxivity of the synthesized polymer PEG-P(Asp (DTPA-Gd)) was as high as 10 $mmol^{-1}$ s^{-1} for 273–26(N10–D5.4–Gd10) and 11 $mmol^{-1}$ s^{-1} for 273–26(N7.4–D5.1–Gd3.2), as shown by closed bars in Fig. 4A and C, respectively. These values were much higher than that of the low molecular weight contrast agent, Gd-DTPA (R_1=5.3 $mmol^{-1}$ s^{-1}). Another polymer 114–44 (N16–D8.9–Gd5.9) in Table 2 showed a relaxivity of 21 $mmol^{-1}$ s^{-1}. This value was higher than that of Gd-DTPA, and those of 273–26(N10–D5.4–Gd10) and 273–26(N7.4–D5.1–Gd3.2), which had a longer PEG chain and a shorter P(Asp) chain than 114–44(N16–D8.9–Gd5.9). In these compositions, the number of bound Gd ions did not influence R_1, but the chain length of the block polymer did significantly change the R_1 values. Although it was well known that T_1 relaxivity of the Gd ions bound to macromolecules was as several times large as that of the corresponding low molecular weight Gd chelate [32,38], few was reported concerning significant change of T_1 relaxivity of macromolecular MRI contrast agents by controlling the number of bound Gd ions per polymer chain and by changing molecular weight in a range of thousands and tens of thousands.

The relaxivity of a mixture of PEG-P(Asp(Gd-DTPA)) and PAA or protamine was revealed to be much lower than that of PEG-P(Asp(DTPA-Gd)). For example, the R_1 value was 2.1 $mmol^{-1}$ s^{-1} for a micelle solution formed from 273–26(N10–D5.4–Gd10) and PAA, and the R_1 value was 2.5 $mmol^{-1}$ s^{-1} for 273–26(N10–D5.4–Gd10) and protamine, as shown by open bars in Fig. 4A and B, respectively. When the number of the chelated Gd was decreased, the R_1 value of the micelle was found to be slightly increased as shown by an open bar in Fig. 4C. The R_1 value of this micelle was still smaller than that of the corresponding low molecular weight chelate, Gd-DTPA. It was found that an addition of NaCl at 150 mM and 500 mM did not influence the T_1 relaxivity of the micelle forming from 273–26(N10–D5.4–Gd10) and PAA.

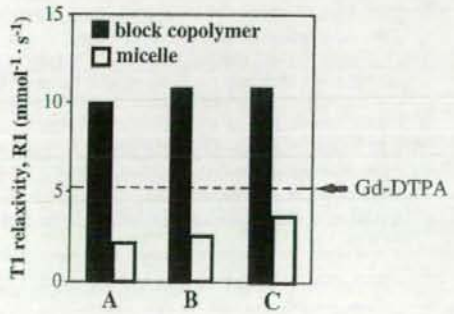

Fig. 4. Effect of micelle formation on relaxivity R_1. (A) 273–26(N10–D5.4–Gd10) and PAA, (B) 273–26(N10–D5.4–Gd10) and protamine, (C) 273–26 (N7.4–D5.1–Gd3.2) and protamine. Block copolymer code is summarized in Table 1. Open bars indicate Gd-containing micelle and closed bars indicate block copolymers only. The relaxivity of Gd-DTPA was shown by dotted line.

These all results indicate that micelle formation lowered the relaxivity of the synthesized polymer PEG-P(Asp-(DTPA-Gd)). This outcome was probably because the Gd that was bound to the PEG-P(Asp) was located in an inner core of the polymer micelle, which was less accessible to water molecules than the outer aqueous environment of the polymeric micelle. We believe that this inner core environment hindered the access of water molecules to the bound Gd ions in the micelle core. In general, Gd-polymer conjugates showed as several times large as T_1 relaxivity values as described above. The T_1 relaxivity values increased due to the limited motion of the polymer-bound Gd ions. These are exemplified by polysaccharide–Gd conjugate [11] (14.1 $mmol^{-1}$ s^{-1} at 20 MHz compared to 3.8 $mmol^{-1}$ s^{-1} of a corresponding low molecular weight Gd chelate), carboxymethyl-dextran–Gd conjugate [10] (10.6 $mmol^{-1}$ s^{-1} at 20 MHz compared to 3.4 $mmol^{-1}$ s^{-1} of a corresponding low molecular weight Gd chelate), polymeric chelate–Gd conjugate [39] (10.1 $mmol^{-1}$ s^{-1} at 20 MHz compared to 3.8 $mmol^{-1}$ s^{-1}), polylysine–Gd conjugate [40] (13.1 $mmol^{-1}$ s^{-1} at 20 MHz compared to 3.7 $mmol^{-1}$ s^{-1}), and albumin–Gd conjugate [41] (20.9 $mmol^{-1}$ s^{-1} at 10.7 MHz compared to 4.9 $mmol^{-1}$ s^{-1}). Although the T_1 relaxivity values are dependent on strength of magnetic field that determines the resonance frequency of proton [12,42], it is noteworthy that the T_1 relaxivity was smaller than that of the corresponding molecular weight chelate in the micelle formation while the T_1 relaxivity of the block copolymer–Gd conjugate was larger than that of the low molecular weight chelate.

All these data proved our hypothesis that the polymeric micelle-type MRI contrast agent possesses an ability to change relaxivity upon micelle formation and dissociation. It was found that the introduction of DTPA-Gd to the block copolymer PEG-P(Asp) increased the Gd's R_1 relaxivity and that the formation of micelle structures decreased the R_1 relaxivity. As illustrated in Fig. 1, through intravenous injection and then through the EPR effect, this polymeric micelle MRI agent can be targeted to solid tumor sites, and this agent provides only a weak contrast of the vascular space during circulation in the blood. After arriving at solid tumor tissues by extravasating the tumor vasculature, this micelle may gradually dissociate into single block copolymer chains. These single block copolymer chains are retained at the solid tumor sites for a long time by the EPR effect and exhibit high MRI contrast. This paper presented the first proof for this strategy. In order to achieve the whole scenario of our novel MRI agent in vivo, researchers must conduct further studies concerning the optimization of (1) micelle diameter, (2) micelle formation stability, and (3) the rate of the dissociation of micelle structures as well as (4) the maximization of the R_1 value of the dissociated block copolymer and (5) the minimization of the R_1

value of the micelle form. In these studies, researchers can undertake these tasks by choosing appropriate compositions of the block copolymer and the cationic polymer.

Acknowledgment

This work was supported by grants from the Ministry of Education, Science, Sports, and Culture, Japan (with a grant No. 10145104 on Priority areas and No. 296, Bio-molecular Design for Biotargeting, and the Program for Promoting the Establishment of Strategic Research Centers, Special Coordination Funds for Promoting Science and Technology) and Grants-in-Aid from the Ministry of Health, Labour and Welfare of Japan.

References

[1] A. Bogdanov Jr., R. Weissleder, In vivo imaging of gene delivery and expression, Trends Biotech. 8 (2002) S11–S18 (Suppl.).
[2] S. Aime, M. Botta, M. Fasano, E. Terreno, Lanthanide(III) chelates for NMR biomedical applications, Chem. Soc. Rev. 27 (1998) 19–29.
[3] T.S. Desser, D.L. Rubin, H.H. Muller, F. Qing, S. Khodor, G. Zanazzi, S.W. Young, D.L. Ladd, J.A. Wellons, K.E. Kellar, J.L. Toner, R.A. Snow, Dynamics of tumor imaging with Gd-DTPA-polyethylene glycol polymers: dependence on molecular, J. Magn. Reson. Imaging 4 (1994) 467–472.
[4] D.M.J. Doble, M. Botta, J. Wang, S. Aime, A. Barge, K.N. Raymond, Optimization of the relaxivity of MRI contrast agents: effect of poly (ethylene glycol) chains on the water-exchange rates of GdIII complexes, J. Am. Chem. Soc. 123 (2001) 10758–10759.
[5] H. Kobayashi, S. Kawamoto, T. Saga, N. Sato, T. Ishimori, J. Konishi, K. Ono, K. Togashi, M.W. Brechbiel, Avidin-dendrimer-(1B4M-Gd)$_{254}$: a tumor-targeting therapeutic agent for gadolinium neutron capture therapy of intraperitoneal disseminated tumor which can be monitored by MRI, Bioconjug. Chem. 12 (2001) 587–593.
[6] H. Kobayashi, S. Kawamoto, S.K. Jo, H.L. Bryant Jr., M.W. Brechbiel, R.A. Star, Macromolecular MRI contrast agents with small dendrimers: pharmacokinetic differences between sizes and cores, Bioconjug. Chem. 14 (2003) 388–394.
[7] S. Langereis, Q.G. Lussanet, M.H.P. Genderen, W.H. Backes, E.W. Meijer, Multivalent contrast agents based on Gadolinium-diethylenetriaminepentaacetic acid-terminated poly(propylene imine) dendrimers for magnetic resonance imaging, Macromolecules 37 (2004) 3084–3091.
[8] V.J. Venditto, C. Aida, M.W. Brechbiel, PANAM dendrimer based macromolecules as improved contrast agents, Mol. Pharmacol. 2 (2005) 302–311.
[9] R. Arebizak, M. Schaefer, E. Dellacherie, Polymeric conjugates of Gd^{3+}-diethylenetriaminepentaacetic acid and dextran: 1. Synthesis, characterization, and paramagnetic properties, Bioconjug. Chem. 8 (1997) 605–610.
[10] C. Corot, M. Schaffer, S. Beaute, P. Bourrinet, S. Zehaf, V. Benize, M. Sabatou, D. Meyer, Physical, chemical and biological evaluations of CMD-A2-Gd-DOTA, Acta Radiol. 38 (Supplement 412) (1997) 91–99.
[11] T.H. Helbich, A. Gossman, P.A. Mareski, B. Raduchel, T.P.L. Roberts, D.M. Shames, M. Muhler, K. Turetschek, R.G. Brasch, A new polysaccharide macromolecular contrast against for MR imaging: biodistribution and imaging characteristics, J. Magn. Reson. Imaging 11 (2000) 694–701.
[12] P. Lebduskova, J. Kotek, P. Hermann, L.V. Elst, R.N. Muller, I. Lukes, J.A. Peters, A gadlinium(III) complex of a carboxylic-phosphorus acid derivative of dietylenetriamine covalently bound to inulin, a potential macromolecular MRI contrast agent, Bioconjug. Chem. 15 (2004) 881–889.
[13] A.M. Mohs, X. Wang, K.C. Goodrich, Y. Zong, D.L. Parker, Z.-R. Lu, PEG-g-poly(GdDTPA-co-L-cystine): a biodegradable macromolecular blood pool contrast agent for MR imaging, Bioconjug. Chem. 15 (2004) 1424–1430.
[14] A. Bogdanov Jr., S.C. Wright, E.M. Marecos, A. Bogdanova, C. Martin, P. Petherick, R. Weissleder, A long-circulating co-polymer in "passive targeting" to solid tumors, J. Drug Target. 4 (1997) 321–330.
[15] H. Kobayashi, N. Sato, T. Saga, Y. Nakamoto, T. Ishimori, S. Toyama, K. Togashi, J. Konishi, M.W. Brechbiel, Monoclonal antibody–dendrimer conjugates enable radiolabeling of antibody with markedly high specific activity with minimal loss of immunoreactivity, Eur. J. Nucl. Med. 27 (2000) 1334–1339.
[16] S.D. Konda, M. Aref, S. Wang, M. Brechbiel, E.C. Wiener, Specific targeting of folate-dendrimer MRI contrast agents to the high affinity folate receptor expressed in ovarian tumor xenografts, Magn. Reson. Mat. Phys. Biol. Med. 12 (2001) 104–113.
[17] K.E. Lokling, S.L. Fossheim, J. Klaveness, R. Skurtveit, Biodistribution of pH-responsive liposomes for MRI and a novel approach to improve the pH-responsiveness, J. Control. Release 98 (2004) 87–95.
[18] M. Mikawa, N. Miwa, M. Brautigam, T. Akaike, A. Maruyama, Gd3+-loaded polyion complex for pH depiction with magnetic resonance imaging, J. Biomed. Mater. Res. 49 (2000) 390–395.
[19] A.Y. Louie, M.M. Huber, E.T. Ahrens, U. Rothbacher, R. Moats, R.E. Jacobs, S.E. Fraser, T.J. Meade, In vivo visualization of gene expression using magnetic resonance imaging, Nat. Biotechnol. 18 (2000) 321–325.
[20] M. Yokoyama, Polymeric micelles for the targeting of hydrophobic drugs, in: G.S. Kwon (Ed.), Polymeric Drug Delivery Systems, Taylor & Francis, Boca Raton, 2005, pp. 533–576.
[21] M. Yokoyama, Drug targeting with polymeric micelle drug carriers, in: N. Yui (Ed.), Supramolecular Design for Biological Applications, CRC Press, Boca Raton, 2002, pp. 245–267.
[22] A. Lavasanifar, J. Samuel, G.S. Kwon, Poly(ethylene oxide)-block-poly(L-amino acid) micelles for drug delivery, Adv. Drug Deliv. Rev. 54 (2002) 169–190.
[23] A.V. Kabanov, V.Y. Alakhov, in: P. Alexandridis, B. Lindman (Eds.), Amphiphilic Block Copolymers: Self Assembly and Applications, Elsevier, Netherlands, 1997, pp. 1–31.
[24] M. Yokoyama, N. Yamada, T. Okano, Y. Sakurai, K. Kataoka, S. Inoue, Toxicity and antitumor activity against solid tumors of micelle-forming polymeric anticancer drug and its extremely long circulation in blood, Cancer Res. 51 (1991) 3229–3236.
[25] G.S. Kwon, S. Suwa, M. Yokoyama, T. Okano, Y. Sakurai, K. Kataoka, Enhanced tumor accumulation and prolonged circulation times of micelle-forming poly(ethylene oxide-aspartate) block copolymer–adriamycin conjugates, J. Control. Release 29 (1994) 17–23.
[26] M. Yokoyama, T. Okano, Y. Sakurai, S. Fukushima, K. Okamoto, K. Kataoka, Selective delivery of adriamycin to a solid tumor using a polymeric micelle carrier system, J. Drug Target. 7 (1999) 171–186.
[27] Y. Matsumura, H. Maeda, A new concept for macromolecular therapeutics in cancer chemotherapy: mechanism of tumoritropic accumulation of proteins and the antitumor agent smancs, Cancer Res. 46 (1986) 6387–6392.
[28] H. Maeda, The enhanced permeability and retention (EPR) effect in tumor vasculature: the key role of tumor-selective macromolecular drug targeting, Adv. Enzyme Regul. 41 (2001) 189–207.
[29] T. Nakanishi, S. Fukushima, K. Okamoto, M. Suzuki, Y. Matsumura, M. Yokoyama, T. Okano, Y. Sakurai, K. Kataoka, Development of the polymer micelle carrier system for doxorubicin, J. Control. Release 74 (2001) 295–302.
[30] T. Hamaguchi, Y. Matsumura, M. Suzuki, K. Shimizu, R. Goda, I. Nakamura, I. Nakatomi, M. Yokoyama, K. Kataoka, T. Kakizoe, NK105, a Paclitaxel-incorporating micellar nanoparticle formulation, can extend the therapeutic window of the drug, Br. J. Cancer 92 (2005) 1240–1246.
[31] J.P. Earls, D.A. Bluemke, New MR imaging contrast agents, Magn. Reson. Imaging Clin. N. Am. 7 (1999) 255–273.
[32] P. Cravan, J.J. Ellison, T.J. McMurry, R.B. Lauffer, Gadolinium (III) chelates as MRI contrast agents: structure, dynamics, and applications, Chem. Rev. 99 (1999) 2293–2352.
[33] M. Yokoyama, G.S. Kwon, T. Okano, Y. Sakurai, T. Seto, K. Kataoka, Preparation of micelle-forming polymer–drug conjugates, Bioconjug. Chem. 3 (1992) 295–301.
[34] E. Gross, J. Meienhofer, The formation of peptide bonds: a general survey, in: E. Gross, J. Meienhofer (Eds.), The Peptides Analysis, Synthesis, Biology, vol. 1, Academic Press, New York, 1980, pp. 65–109.
[35] V. Saudek, H. Pivcova, J. Drobnik, NMR study of poly(aspartic acid): II. α- and β-peptide bonds in poly(aspartic acid) prepared by common methods, Biopolymers 20 (1981) 1615–1623.

[36] A.P. Pathak, B. Bimi, K. Glunde, E. Ackerstaff, D. Artemov, Z.M. Bhujwalla, Molecular and functional imaging of cancer: advances in MRI and MRS, Methods Enzymol. 386 (2004) 3–60.
[37] Z.R. Lu, X. Wang, D.L. Parker, K.C. Goodrich, H.R. Buswell, Poly(L-glutamic acid) Gd(III)–DOTA conjugate with a degradable spacer for magnetic resonance imaging, Bioconjug. Chem. 14 (2003) 715–719.
[38] R. Mathur-de-Vre, M. Lemort, Invited review: biophysical properties and clinical applications of magnetic resonance imaging contrast agents, Br. J. Radiol. 68 (1995) 225–247.
[39] D.L. Ladd, R. Hollister, X. Peng, D. Wei, G. Wu, D. Delecki, R.A. Snow, J. Toner, K. Kelar, J. Eck, V.C. Desai, G. Raymond, L.B. Kinter, T.S. Desser, D.M. Rubin, Polymeric gadolinium chelate magnetic resonance imaging contrast agents: design, synthesis, and properties, Bioconjug. Chem. 10 (1999) 361–370.
[40] G. Schuhmann-Giampieri, H. Schmitt-Willich, T. Frenzel, W.-R. Press, H.-J. Weinmann, In vivo and in vitro evaluation of Gd-DTPA-polylysine as a macromolecular contrast agent for magnetic resonance imaging, Invest. Radiol. 26 (1991) 969–974.
[41] M.G. Wikstrom, M. Moseley, D. White, J.W. Dupon, J. Winkelhake, J. Kopplin, R.C. Brasch, Contrast-enhanced MRI of tumors comparison of Gd-DTPA and a macromolecular agent, Invest. Radiol. 24 (1989) 609–615.
[42] A. Accardo, D. Tesauro, P. Roscigno, E. Gianolio, L.D. Paduano, G. Errico, C. Pedone, G. Morelli, Physicochemical properties pf mixed micellar aggregates containing CCK peptides and Gd complexes designed as tumor specific contrast agents in MRI, J. Am. Chem. Soc. 126 (2004) 3097–3107.

Available online at www.sciencedirect.com
ScienceDirect
Journal of Controlled Release 115 (2006) 46–56
journal of controlled release
www.elsevier.com/locate/jconrel

Molecular design of biodegradable polymeric micelles for temperature-responsive drug release

Masamichi Nakayama [a], Teruo Okano [a,*], Takanari Miyazaki [b], Fukashi Kohori [b], Kiyotaka Sakai [b], Masayuki Yokoyama [c,*]

[a] Tokyo Women's Medical University, Institute of Advanced Biomedical Engineering and Science, Kawada-cho 8-1, Shinjuku-ku, Tokyo 162-8666, Japan
[b] Waseda University, Department of Applied Chemistry, 3-4-1, Ohkubo, Shinjuku-ku, Tokyo 169-8555, Japan
[c] Kanagawa Academy of Science and Technology, Yokoyama "Nano-medical polymers" project, KSP East 404, Sakado 3-2-1, Takatsu-ku, Kawasaki-shi, Kanagawa 213-0012, Japan

Received 27 March 2006; accepted 10 July 2006
Available online 14 July 2006

Abstract

We designed thermo-responsive and biodegradable polymeric micelles for an ideal drug delivery system whose target sites are where external stimuli selectively release drugs from the polymeric micelles. The thermo-responsive micelles formed from block copolymers that were composed both of a hydrophobic block and a thermo-responsive block. Poly(*N*-isopropylacrylamide-co-*N*,*N*-dimethylacrylamide) showing a lower critical solution temperature (LCST) around 40 °C was synthesized for the thermo-responsive block, while biodegradable poly(D,L-lactide), poly(ε-caprolactone), or poly(D,L-lactide-co-ε-caprolactone) was used for the hydrophobic block. By changing both the block lengths of the poly(D,L-lactide)-containing block copolymers, physical parameters such as micelle diameter and critical micelle concentration were varied. On the other hand, the choice of the hydrophobic block was revealed to be critical in relation to both on the thermo-responsive release of the incorporated anti-cancer drug, doxorubicin, and the temperature-dependent change of the hydrophobicity of the micelles' inner core. One polymeric micelle composition successfully exhibited rapid and thermo-responsive drug release while possessing a biodegradable character.

Keywords: Polymeric micelle; Biodegradable polymer; Thermo-response; Temperature; Targeting

1. Introduction

Drug targeting has attracted much attention not only in basic science but also in clinical medicine, particularly for cancer chemotherapy [1,2]. Since the 1990s, many clinical trials have been conducted for the targeting systems of anti-cancer drugs, and some of them are currently approved for clinical use.

Drug targeting is defined as selective drug delivery to specific sites, organs, tissues or cells where drug activities are required. Drug targeting includes two components: (1) selective delivery to the target sites and (2) drug release from drug carriers at the target sites. The selective delivery (by intravenous injection, in many cases) can be achieved by drug conjugation or drug incorporation to or into appropriate drug carriers. The drug carriers include natural polymers (e.g., antibodies [3–5], transferrin [6,7], synthetic polymers [8–11], emulsions [12,13] micro(nano) particles [14,15], liposomes [16,17], and polymeric micelles [18–26]). The other important component of drug targeting is drug release, whose importance derives from the following phenomenon: a drug can express its pharmacological activities only after its release from the carriers in many cases, and therefore, even if the selective delivery is achieved, the realization of better therapeutic effects must include drug release that follows an appropriate rate and an appropriate timing. In an ideal drug targeting system, the drug is not released during its delivery from the injection site to its therapeutic targets — which is to say, the

* Corresponding authors. Yokoyama is to be contacted at Kanagawa Academy of Science and Technology, Yokoyama "Nano-medical polymers" project KSP East 404, Sakado 3-2-1, Takatsu-ku, Kawasaki-shi, Kanagawa 213-0012, Japan. Tel.: +81 44 819 2093; fax: +81 44 819 2095. Okano, Tokyo Women's Medical University, Institute of Advanced Biomedical Engineering and Science, Kawada-cho 8-1, Shinjuku-ku, Tokyo 162-8666, Japan.
E-mail address: masajun@ksp.or.jp (M. Yokoyama).

0168-3659/$ - see front matter © 2006 Elsevier B.V. All rights reserved.
doi:10.1016/j.jconrel.2006.07.007

drug is not released in the bloodstream; rather, the drug is released selectively at the targets.

One way to achieve the selective drug targeting and release is stimulus-responsive drug release. Stimuli that are specific at target sites may include low pH, high levels of certain enzymes, and externally applied physical signals (e.g., high temperature, light, magnetic field, and ultrasound). Among these internal and external stimuli, high temperature is one of the best signals in terms of easy and safe medical applications. The merits of high temperature are due to the substantial strides that medical researchers have made in applications of the hyperthermia therapy to solid tumors.

For temperature-responsive drug release systems, two types of carrier systems have been studied: thermo-responsive liposomes [27,28] and thermo-responsive polymeric micelles [29]. Over the last five years, we [30–36] and others [37–39] have investigated this carrier system mainly because (1) polymeric micelle carrier systems have advantages in the incorporation of water-insoluble drugs [40,41], and (2) many potent drugs have been water-insoluble. The thermo-responsive liposomes are not suitable for the incorporation of water-insoluble drugs. As shown in Fig. 1, the formation of a thermo-responsive polymeric micelle results from the assembly of block copolymers composed of a thermo-responsive block and a hydrophobic block. Drug molecules are incorporated into the hydrophobic inner core, and the thermo-responsive characfer is possessed by the outer shell of the polymeric micelles. When the temperature is below the phase-transition temperature of the thermo-responsive block, micelles are formed with the hydrated outer shell and the hydrophobic inner core. When the temperature exceeds the phase-transition temperature, the outer shell shrinks and becomes hydrophobic. Intermicellar aggregates may form on the basis of both a micelle concentration and the strength of the shrunken outer shell layer's hydrophobic interactions. A rise in temperature may enhance the drug release.

Poly(*N*-isopropylacrylamide) (P(IPAAm)) is the most widely used synthetic temperature-responsive material not only in drug delivery but also in biomaterial studies and intelligent material studies such as those that concern hydrogels [42,43] and bioconjugates [44]. One strong reason for the frequent use of this polymer is that its phase-transition occurs approximately at the body temperature. P(IPAAm) is known to exhibit phase-transition at 32 °C in water, and for the purposes of drug targeting scientist can adjust this phase-transition temperature to an appropriate temperature (around 40 °C) by introducing a hydrophilic comonomer such as *N*,*N*-dimethylacrylamide (DMAAm).

In previous reports, we prepared thermo-responsive polymeric micelles whose formation resulted from the block copolymers that, for the outer shell, were composed of a thermo-responsive P(IPAAm) block or a P(IPAAm-co-DMAAm) block and that, for the drug-incorporated inner core, were composed of a hydrophobic poly(D,L-lactide) (PLA) block [32,34–36] or a poly(butyl methacrylate) block [30,31,33,35]. We also reported temperature-responsive changes that affected (1) the polymeric micelles' physico-chemical characteristics [30–32,35] and (2) the thermo-responsive drug release [33–35] and the cytotoxic actions to cultured cells [33,34]. Biodegradable properties are considered preferable for micelle-forming block copolymers, since polymers obtained after degradation of the hydrophobic block are expected to be quickly excreted in the kidney if a molecular weight of the thermo-responsive block is designed below the critical value (approx. 40,000) for the renal excretion [45]. For the polymeric micelles containing the poly(butyl methacrylate) block, rapid and thermo-responsive drug release was obtained. However, this block copolymer is not biodegradable. For the polymeric micelle system using PLA as the hydrophobic block, we achieved significant enhancements in drug release and cytotoxicity [34]. However, the obtained drug-release rate was too low for strong cytotoxic action (only 15% release in 6 days when the temperature exceeded the phase-transition temperature).

In this paper, we try to obtain an appropriate design of thermo-responsive polymeric micelles by using PLA or other biodegradable polyesters for both quick drug release and sharp

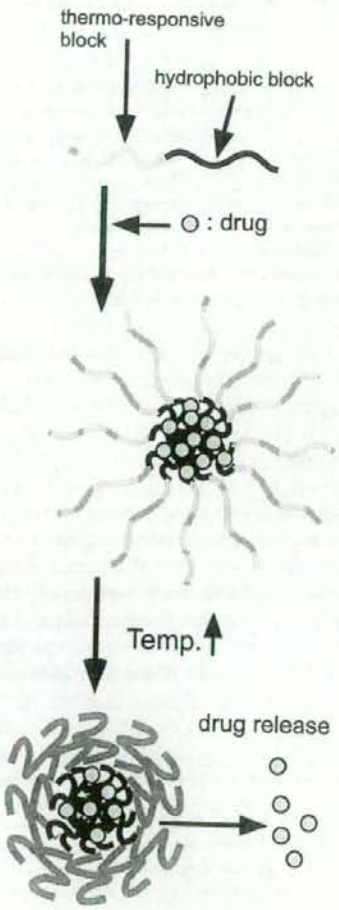

Fig. 1. Thermo-responsive polymeric micelle for selective drug release when the temperature rises.

thermo-responsiveness. Indeed, by using various chain lengths of both the thermo-responsive block and the hydrophobic block and by using PLA and poly(ε-caprolactone) (PCL) in the hydrophobic block, we have tried to identify essential factors that underlie a design for biodegradable polymeric micelles whose drug release behavior is preferable for clinical use.

2. Materials and methods

2.1. Materials

N-Isopropylacrylamide (IPAAm) was kindly provided from Kohjin (Tokyo, Japan) and recrystallized from *n*-hexane. *N,N*-Dimethylacrylamide (DMAAm) and ε-caprolactone (CL) were purchased from Wako Pure Chemicals (Osaka, Japan) and were purified via reduced-pressure distillation. D,L-Lactide (TCI, Tokyo, Japan) was purified via recrystallization from ethyl acetate. Tetrahydrofuran (THF), 2-mercaptoethanol and xylene were purchased from Wako Pure Chemicals (Osaka, Japan). THF was dried via reflux with CaH_2 and was fractionally distilled. Xylene was dried with molecular sieves 3A (Wako Pure Chemicals, Osaka, Japan). Benzoyl peroxide (BPO), *N,N*-dimethylacetamide (DMAC) (Kanto Chemical Co., Inc., Tokyo, Japan), tin(II) 2-ethylhexanoate (Sn(OCt)2), triethylamine (TEA), *N,N*-dimethylformamide (DMF), and lithium chloride (LiCl) were purchased from Wako Pure Chemicals and used in their purchased state.

2.2. Polymer syntheses

Block copolymers were obtained along the synthetic routes shown in Scheme 1.

2.2.1. Synthesis of hydroxy-terminated P(IPAAm-co-DMAAm) (3)

N-isopropylacrylamide (IPAAm, **1**) and dimethylacrylamide (DMAAm, **2**) were copolymerized in the presence of a chain-transfer agent (2-mercaptoethanol) that was used for the introduction of a hydroxyl group at one terminal of the copolymer. The dissolution of IPAAm and DMAAm in tetrahydrofuran (THF) preceded additions of benzoyl peroxide (BPO) and 2-mercaptoethanol. The mixed solution was degassed via three freeze–thaw cycles in vacuo. We carried out the polymerization with stirring at 70 °C for 7 h. The polymerization was terminated by the introduction of air into this reaction flask. Approximately a half volume of the solvent was evaporated in vacuo, and then the solution was poured into a large excess of diethyl ether. The precipitated polymer was filtrated and washed with ether. Precipitation was repeated twice with acetone and diethyl ether for good and poor solvents, respectively, and was followed by drying in vacuo. The product was obtained as white powder. The composition of the copolymer was determined by ^{1}H NMR spectroscopy. Peaks of both a side chain methine proton ($-NHCH(CH_3)_2$) of the IPAAm unit at 4.0 ppm and a methyl proton ($-N(CH_3)_2$) of the DMAAm unit at 3.0 ppm were used for this determination. The weight average molecular weight and the Mw/Mn ratio were measured by GPC.

2.2.2. Fractionation of hydroxy-terminated P(IPAAm-co-DMAAm) (3)

Fractionation of the hydroxy-terminated P(IPAAm-co-DMAAm) (**3**) was carried out in two ways: by ultrafiltration and gel-filtration.

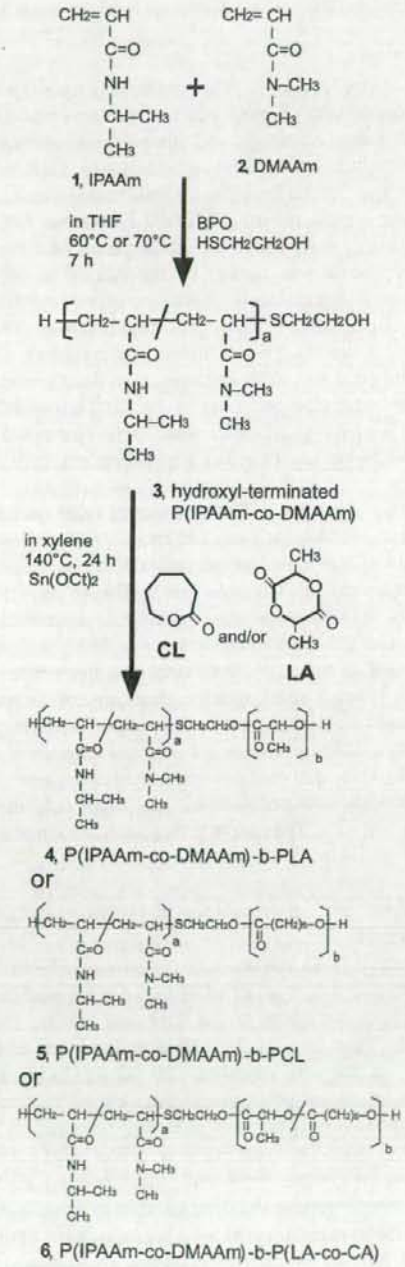

Scheme 1. Syntheses of block copolymers.

Table 1
Synthesis of hydroxy-terminated P(IPAAm-co-DMAAm) (3)

Run	IPAAm	DMAAm	2-mercapto-ethanol	BPO	Reaction	THF	Molar ratio IPAAm/DMAAm		Yield	Mw	Mw/Mn[1)]
							feed	found			
1	28.18 g(249 mmol)	5.06 g (51 mmol)	0.469 g (6.0 mmol)	0.121 g (0.50 mmol)	70 °C 7 h	100 ml	83/17	78/22	10.28 g 30.5%	1.38×10^4	2.49
2	32.59 g (288 mmol)	7.14 g (72 mmol)	0.563 g (7.2 mmol)	0.146 g (0.60 mmol)	60 °C 7 h	120 ml	80/20	n.d.	8.36 g 20.7%	1.00×10^4	2.73

[1)]Determined by GPC. Mw: weight-averaged molecular weight, Mn: number-averaged molecular weight.

2.2.2.1. Ultrafiltration. The synthesized hydroxy-terminated P(IPAAm-co-DMAAm) (**3**, run 1 of Table 1) was dissolved in distilled water (1.5 wt.%), and this polymer solution was fractionated with two ultrafiltration membranes. First, the polymer solution was filtered through an ultrafiltration membrane with a molecular weight cut-off of 20,000 (Advantec UK-20, Toyo Roshi Kaisha, Ltd., Tokyo Japan). In the second step, the thus obtained filtrate was filtered by the use of an ultrafiltration membrane with a molecular weight cut-off of 10,000 (Advantec UK-10, Toyo Roshi Kaisha, Ltd., Tokyo Japan). The residual solution on the UK-10 membrane was collected and lyophilized. The yield was 47%. The average molecular weight of this fractionated polymer was found to be 12,200 by GPC, and this polymer's ratio of Mw/Mn was 1.44. The results of this fractionation are shown in run 1 of Table 2.

2.2.2.2. Gel-filtration. The synthesized hydroxy-terminated P(IPAAm-co-DMAAm) (**3**, run 2 of Table 1, 6.75 g) was dissolved in 67.5 ml of *N,N*-dimethyformamide (DMF) containing 10 mM LiCl. Toyopearl HW-50 gel (Tosoh, Tokyo, Japan) that was suspended in DMF containing 10 mM LiCl was packed in a glass column. The gel bed-volume was 1.5 L. The polymer solution was applied to this HW-50 column, and three fractions were collected. Using a Spectrapor 6 dialysis membrane (molecular-weight cut-off: 1000, Spectrum Laboratories, Inc., Rancho Dominguez, CA) for 2 days, we dialyzed these three collected fractions were dialyzed against distilled water. We then lyophilized the obtained solution. The total yield of the three fractions was 43%. The results of this fractionation are shown in runs 2–4 of Table 2.

2.2.3. Synthesis of P(IPAAm-co-DMAAm)-b-PLA block copolymer (**4**)

D,L-Lactide (LA) and the hydroxy-terminated P(IPAAm-co-DMAAm) polymer were dried in vacuo for 2 h at 50 °C in a flask. Xylene was added to this flask, and the substrates were dissolved. Then, tin(II) 2-ethylhexanoate was added. The reaction mixture was stirred at 150 °C for 24 h. Then, the reaction mixture was poured into a large excess of diethyl ether. The precipitated polymer was collected, filtrated, and washed with diethyl ether. The resulting product was dried in vacuo. We determined the compositions of the block copolymers by using ^{1}H NMR spectroscopy. The determination was made by the use of both a methine proton peak (–COC*H*(CH_3)O–) of the lactide unit at 5.1 ppm and a side chain methine proton peak (–NHC*H*(CH_3)$_2$) of the IPAAm unit at 4.0 ppm.

2.2.4. Syntheses of P(IPAAm-co-DMAAm)-b-PCL block copolymer (**5**) *and P(IPAAm-co-DMAAm)-b-poly(LA-co-CL) block copolymer* (**6**)

The hydroxy-terminated P(IPAAm-co-DMAAm) polymer (**3**) and ε-caprolactone (CL) were dried in vacuo for 2 h at 50 to 60 °C in a flask. D,L-Lactide (LA) was also dried with the polymer and CL for a synthesis of P(IPAAm-co-DMAAm)-b-poly(LA-co-CL) (**6**). Xylene was added to the flask, and the substrates were dissolved. Then, tin(II) 2-ethylhexanoate was added. The reaction mixture was stirred at 140 °C for 24 h. Then, the reaction mixture was poured into a large excess of diethyl ether. After being collected, filtrated, and washed with diethyl ether, the precipitated polymer was dried in vacuo. We determined the compositions of the block copolymers were by using ^{1}H NMR spectroscopy. The determination was made by the use of a methine proton peak (–COC*H*(CH_3)O–) of the LA unit at 5.1 ppm, a methylene proton peak (–COCH_2CH_2CH_2-CH_2CH_2O–) of the CL unit at 2.3 ppm, and a side chain methine proton peak (–NHC*H*(CH_3)$_2$) of the IPAAm unit at 4.0 ppm.

2.3. Fluorescence measurements

Fluorescence spectra were recorded on a spectrofluorometer (FP-770, Japan Spectroscopic Co., Ltd., Tokyo, Japan). The temperature of a water-jacketed cell holder was controlled with a Peltier-effect cell holder. Pyrene was used as a hydrophobic fluorescent probe. Unless otherwise stated, a pyrene solution in acetone (2×10^{-4} M) was added to aqueous polymer solutions at the final pyrene concentration of 6×10^{-7} M. These samples containing pyrene were stirred for 24 h at room temperature for

Table 2
Fractionated hydroxy-terminated P(IPAAm-co-DMAAm) (3)

Run	Polymer	Method	Average Mw[1)]	Mw/Mn[1)]	IPAAm/DMAAm ratio[2)]	Yield (%)
1	Run 1 of Table 1	Ultrafiltration	12,200	1.44	n.d.	47.1
2	Run 2 of Table 1	Gel-filtration	10,800	1.46	68:32	11.7
3	Run 2 of Table 1	Gel-filtration	17,000	1.65	74:26	16.7
4	Run 2 of Table 1	Gel-filtration	28,500	1.79	72:28	14.5

[1)]Determined by GPC. Mw: weight-averaged molecular weight, Mn: number-averaged molecular weight.
[2)]Determined by ^{1}H NMR.

Table 3
Synthesis of P(IPAAm-co-DAAm)-b-PLA block copolymer (4)

Run	Hydroxy-terminated P(IPAAm-co-DMAAm), 3	D,L-lactide	Tin(II) 2-ethyl-hexanoate	Xylene	Yield	M.W.[1] of P (IPAAm-co-DMAAm) block	M.W.[2] of PLA block	M.W.[3] and Mw/Mn[4] of block copolymer	Cumulant average diameter of micelle (nm)	LCST (°C)
1	Run 1 of Table 2 0.50 g	0.25 g	75.1 mg	0.5 ml	0.45 g 60.4%	12,200	1400	1.68×10^4 1.32	34.5	41.5
2	Run 1 of Table 2 0.50 g	0.50 g	75.1 mg	1.0 ml	0.58 g 57.5%	12,200	2600	1.98×10^4 1.35	49.2	41.0
3	Run 1 of Table 2 0.50 g	1.00 g	75.1 mg	2.0 ml	0.82 g 54.5%	12,200	6100	2.46×10^4 1.33	69.2	40.5
4	Run 2 of Table 2 0.70 g	0.64 g	36.2 mg	5.3 ml	0.83 g 62.0%	10,800	5900	1.61×10^4 1.55	41.3	39.0
5	Run 3 of Table 2 1.00 g	0.75 g	50.0 mg	7.5 ml	1.22 g 69.6%	17,000	6600	2.14×10^4 1.63	47.9	39.5
6	Run 4 of Table 2 0.80 g	0.43 g	43.0 mg	6.0 ml	0.87 g 70.7%	28,500	7300	3.30×10^4 1.70	48.7	40.0

[1]Weight-averaged molecular weight determined by GPC.
[2]Number-averaged molecular weight determined by ^{1}H NMR by the use of M.W. of P(IPAAm-co-DMAAm) block.
[3]Weight-averaged molecular weight determined by GPC.
[4]Mw/Mn=weight-averaged molecular weight/number-averaged molecular weight determined by GPC.

the complete evaporation of acetone. The polymer concentration was 5 mg/ml. Excitation was carried out at 340 nm. The emission spectra were recorded in a range from 350 to 600 nm. Excitation and emission band widths were 10 nm and 3 nm, respectively. From the pyrene emission spectra, the intensity (peak height) ratios (I_1/I_3) of the first band (374 nm) to the third band (385 nm) were analyzed as a function of either polymer concentrations or temperature. For the measurements in Fig. 5, we also incorporated pyrene into the micelles' hydrophobic inner core by the two other methods. These two methods are described below.

2.3.1. Dialysis method

After dissolving pyrene and a block copolymer in DMAC, we dialyzed this mixed solution against distilled water by using a dialysis membrane with a 12,000 to 14,000 molecular-weight cut-off (Spectra/Por®2, Spectrum Medical Industries, Inc., CA, USA) at 25 °C. An amount of used pyrene was set at the final pyrene concentration in the aqueous solution of 6×10^{-7} M. A concentration of the block copolymer was 5 mg/ml.

2.3.1.1. Evaporation method from chloroform. Pyrene and a block copolymer were dissolved in chloroform in a glass tube. This solution was stirred with a magnetic stirrer in a N_2 gas flow. The chloroform was completely evaporated at room temperature. The addition of distilled water to this glass tube was followed by sonication for 2 min. This sonication was done with a probe-type sonicator model VC 100 (Sonics and Materials Inc., Connecticut, USA) equipped with a standard 6 mm probe. For this sonication, the cycle was set at 0.5 s and standby at 0.5 s. Concentrations of pyrene and the block copolymer were 6×10^{-7} M and 5 mg/ml, respectively.

2.4. Incorporation of an anticancer drug, doxorubicin, into polymeric micelles forming from block copolymers

Both drug loading in the inner cores of micelles and preparation of micelles were simultaneously carried out on the basis of a dialysis method, as reported previously [36]. Doxorubicin hydrochloride (DOX·HCl, 15.0 mg) was dissolved in *N,N*-dimethylacetamide (DMAC, 7.5 ml), and triethylamine (TEA, 1.5 mol eq. to DOX·HCl) as added to this solution. A block copolymer (15.0 mg) was dissolved in 7.5 ml of DMAC. The room-temperature mixing of the DOX solution and the block copolymer solution was followed by dialysis against distilled water. This dialysis involved the use of a dialysis membrane with a 12,000 to 14,000 molecular-weight cut-off (Spectra/Por®2, Spectrum Medical Industries, Inc., CA, USA) at 25 °C. Then, the polymeric micelle solutions were concentrated via ultrafiltration that featured a membrane with a molecular-weight cut-off of 200,000 (Ultrafilter Q2000, Advantec Toyo Kaisha, Ltd. Tokyo, Japan).

2.5. Drug release from polymeric micelles

Polymeric micelle solutions (5 ml) were put in a dialysis tube (Spectra/Por®2, 12,000 to 14,000 molecular-weight cut-off, Spectrum Medical Industries, Inc., CA, USA) placed in 100 ml of Dulbecco's phosphate-buffered saline (PBS) at pH 7.4. The initial DOX concentration of the micelles was 30 μg/ml. The temperature of the experimental system was set at 35 °C or 41 °C. Occasionally, a small amount of the inner solution was taken, and its DOX content was measured via absorbance at 485 nm.

2.6. Other measurements

The molecular weights (M.W.) of the polymers were determined by gel-permeation chromatography (GPC, Tosoh, SC-8020, poly(ethylene glycol) standards) in DMF that contained LiCl (10 mM) (elution rate: 1.0 ml/min). This chromatography system was equipped with either TSKgel G-3000 H_{HR}+TSKgel G-4000H_{HR} columns or TSKgel α-3000+TSKgel α-4000 columns at 40 °C. Doxorubicin (DOX) concentrations were measured in relation to visible light absorbance at 485 nm. To execute these measurements, we used a UV–VIS spectrometer (V-530, Japan Spectroscopic Co., Ltd., Tokyo, Japan). For micelles (5 mg/ml) that were in Dulbecco's phosphate-buffered saline (PBS) and that were at various temperatures, optical transmittance was measured at 500 nm. The measurements derived from the same UV–VIS spectrometer. The sample cell was thermostated with a Peltier-effect cell holder (EHC-477, Japan Spectroscopic Co.,

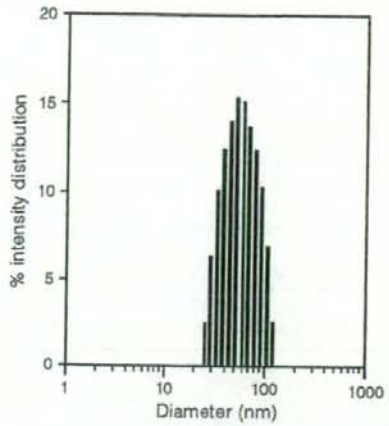

Fig. 2. Diameter distribution of polymeric micelles forming from P(IPAAm-co-DMAAm)-b-PLA, run 3 in Table 2.

Ltd., Tokyo, Japan). The heating rate was 0.1 °C/min. A lower critical solution temperature (LCST) of the micelle was determined at a temperature showing 50% transmittance. To measure the diameters of the micelles, we relied on dynamic light scattering, for which we used a DLS-7000 instrument (Otsuka Electronics Co., Ltd., Osaka, Japan) equipped with a He–Ne or Argon laser and analyzed by the Cumulant method. Light scattering intensity measurements for the critical micelle concentration determination were carried out in the static light scattering mode of the same instrument. Before conducting these light scattering measurements, we filtered samples through a 0.45 μm filter (Samprep LCR13-LH, Nihon Millipore Ltd., Tokyo, Japan). We measured the glass transition temperatures of block copolymers by using a differential scanning calorimeter DSC 8230 (Rigaku Corp., Tokyo, Japan). The polymeric micelle solutions were obtained by the above described dialysis method, and were freeze-dried. Thus obtained freeze-dried samples (approximately 3 to 8 mg) were measured in aluminum sample cells.

3. Results and discussion

3.1. Synthesis and fractionation of hydroxy-terminated P(IPAAm-co-DMAAm) (3)

Hydroxy-terminated P(IPAAm-co-DMAAm) was synthesized according to the reported method [32,36]. *N*-Isopropylacrylamide (IPAAm) was copolymerized with *N*,*N*-dimethylacrylamide (DMAAm) for the syntheses of block copolymers possessing phase-transition temperatures around 40°C. This transition temperature is useful for temperature-induced drug release in living bodies. As summarized in Table 1, our polymerization involved monomer feed ratios of 83:17 and 80:20 (the major component was IPAAm) for run 1 and run 2, respectively. Using 2-mercaptoethanol as a chain-transfer agent, copolymers with average molecular weights of 13,800 and 10,000 were obtained in run 1 and run 2, respectively. Because these copolymers had considerably wide molecular weight distributions, as shown by the Mw/Mn ratios over 2.4, their fractionation was carried out.

For copolymer run 1, we conducted ultrafiltration, which yielded the average molecular weight of 12,200 and the Mw/Mn ratio of 1.44. This fractionated copolymer (run 1 of Table 2) was used for syntheses of P(IPAAm-co-DMAAm)-b-PLA block copolymers possessing various PLA block lengths (runs 1 through 3 of Table 3).

For copolymer run 2 of Table 1, we conducted gel-filtration to obtain copolymer fractions that exhibited considerably narrow molecular weight distributions. We obtained (as summarized in Table 2) three fractions that had the average molecular weights of 10,800, 17,000, and 28,500 and that had considerably narrow molecular weight distributions under 1.80 for the Mw/Mn ratio in runs 2, 3, and 4 of Table 2, respectively. These three fractions were used for syntheses of P(IPAAm-co-DMAAm)-b-PLA block copolymers possessing various P(IPAAm-co-DMAAm) block lengths and almost the same PLA block lengths.

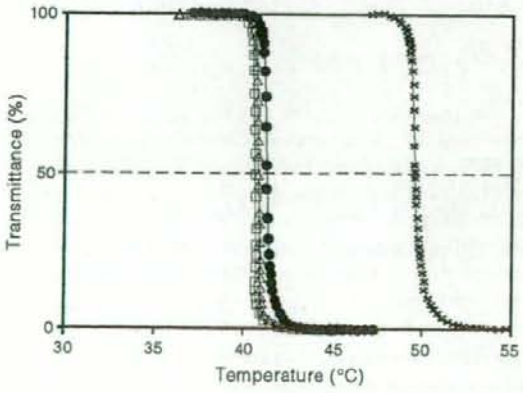

Fig. 3. LCST determination of P(IPAAm-co-DMAAm)-b-PLA. Transmittance at 500 nm was measured in phosphate-buffered saline at pH 7.4. The temperature rate-of-increase was 0.1 °C per min. ●: run 1 of Table 3, Δ: run 2 of Table 3, ❑: run 3 of Table 3. ×: P(IPAAm-co-DMAAm) run 1 of Table 2.

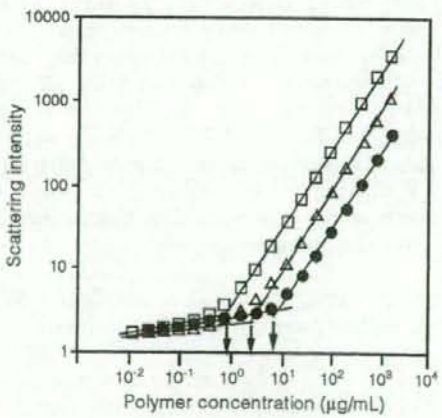

Fig. 4. Light-scattering intensity measurements by the static-light-scattering mode of P(IPAAm-co-DMAAm)-b-PLA in distilled water for CMC determination. ●: run 1 of Table 3, Δ: run 2 of Table 3, ❑ : run 3 of Table 3.

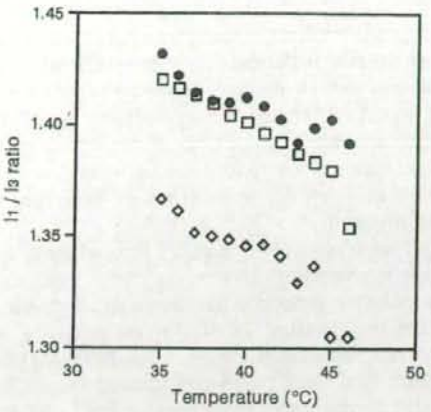

Fig. 5. Comparison of pyrene fluorescence spectra based on three different pyrene incorporation methods. The block copolymer was P(IPAAm-co-DAAm)-b-PLA block copolymer run 4 in Table 3 at a concentration of 5 mg/ml. ●: acetone method, ◇: dialysis method, and ❑: chloroform-evaporation method.

3.2. Syntheses of P(IPAAm-co-DMAAm)-b-PLA block copolymers (4) and their micelle-formation behaviors

The results of P(IPAAm-co-DMAAm)-b-PLA block copolymer syntheses are summarized in Table 3. Runs 1 through 3 were obtained from the identical hydroxy-terminated P(IPAAm-co-DMAAm) (3), run 1 of Table 2. These three block copolymers possessed different molecular weights of the PLA block that ranged from 1400 to 6100. In GPC measurements, we observed a complete shift of the block copolymer peaks from the hydroxy-terminated P(IPAAm-co-DMAAm) for these three block copolymers. These were single peaks and were not accompanied by a shoulder peak of the residual hydroxy-terminated P(IPAAm-co-DMAAm). For these three runs, we found that polymeric micelles formed according to the dialysis method, and that no precipitation accompanied this micelle formation. Fig. 2 shows a result of the dynamic light scattering measurement of run 3. The observed unimodal and narrow distribution indicates successful micelle preparation without any secondary associate. The average micelle diameter was observed to be larger for the block copolymer possessing the longer hydrophobic PLA block, as summarized in Table 3. Fig. 3 shows results of the phase-transition temperature measurements. The hydroxy-terminated P(IPAAm-co-DMAAm), which was a precursor of the block copolymers runs 1 through 3, exhibited the lower critical solution temperature (LCST) at 49.0 °C. This LCST was found to shift considerably to the lower temperature side when the hydrophobic PLA chain attached itself to the P(IPAAm-co-DMAAm) terminal. The LCSTs of runs 1 through 3 in the phosphate-buffered saline were almost identical around 41 °C, even though the block copolymer that possessed the longer hydrophobic block showed the slightly higher LCST. We considered that the terminal hydrophilic hydroxyl group substantially raised the LCST of the P(IPAAm-co-DMAAm) copolymer, and that the P(IPAAm-co-DMAAm) copolymer recovered its original phase-transition temperature owing to the conversion of the hydroxyl group to a more hydrophobic ester group in the block copolymers. These outcomes indicate that the precise control of the transition temperature fell uniquely to the composition control of the P(IPAAm-co-DMAAm) chain, and that the chain length of the PLA block did not influence the transition temperature.

To synthesize the block copolymer runs 4 through 6 in Table 3, we used various chain lengths of the P(IPAAm-co-DMAAm). The chain lengths of the hydrophobic PLA block of these three copolymers were almost the same, measuring between 6000 and 7000, approximately. According to our observations, these three block copolymers formed polymeric micelle structures without any secondary association (data not shown). This formation was similar in manner to run 3, as shown in Fig. 2. Furthermore, we observed that these micelles possessed LCSTs around 39.5 °C in PBS. The Cumulant average micelle diameters of these runs ranged from 40 to 50 nm. These numbers are considered appropriate for targeting solid tumors. As stated above, the thermo-responsive polymeric micelles having various chain lengths both of the thermo-responsive block and the hydrophobic block were successfully synthesized. These micelles had appropriate diameters and LCSTs.

A critical micelle concentration (CMC) is a fundamental parameter describing the physico-chemical characteristics of polymeric micelles, and this parameter is considered important for drug targeting applications, since single block copolymer chains that do not form any micellar structure are considered to be very different from polymeric micelles in delivery behaviors in the bloodstream. This perceived difference is due to the significant difference in size between the single polymer and the polymeric micelle. In general, scientists determine the CMC of a polymeric micelle by relying on a fluorescence method that features pyrene as a fluorescence probe [46]. A polymer concentration showing a discontinuous change in fluorescence intensity or in an intensity ratio between the first and third bands

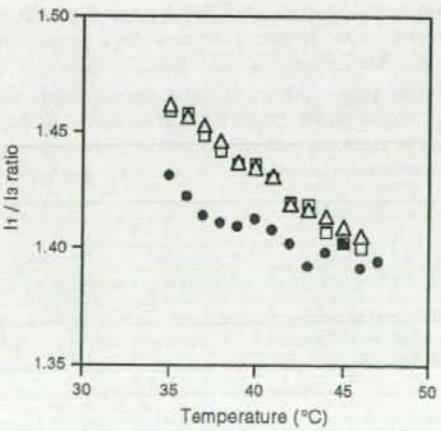

Fig. 6. Fluorescence of pyrene incorporated into polymeric micelles forming from P(IPAAm-co-DMAAm)-b-PLA. ●: run 4 of Table 3, Δ: run 5 of Table 3, and ❑: run 6 of Table 3.

of an emission spectrum of pyrene is defined as the CMC. However, this pyrene fluorescence method is based on the assumption that pyrene is freely distributed in a hydrophobic inner core of the polymeric micelle, and that this distribution stems from an addition of pyrene solution (usually acetone solution). If the rigid character of the inner core inhibits this uniform pyrene distribution, the results obtained through this pyrene method do not provide a true CMC value. We were afraid that this possibility might manifest itself in our research because the PLA exhibits a notably rigid character at room temperature. The room temperature is below its glass transition temperature (ca. 55 °C). Therefore, we relied on static light scattering to measure the scattering intensities of block copolymer solutions at various concentrations. Fig. 4 shows results for P(IPAAm-co-DMAAm)-b-PLA block copolymers runs 1 through 3 of Table 3. All three polymers showed discontinuous changes in the scattering intensities plotted against polymer concentrations. The concentrations showing the discontinuous changes were defined as CMC, and the thus obtained CMC values ranged from 1 through 9 μg/ml. These CMC values were found to be smaller for the block copolymer that possessed the longer PLA chain and to agree well with CMC values that we measured according to the pyrene fluorescence method. For example, in relation to both our light scattering method and our fluorescence method, we obtained 1 μg/ml for run 1. This indicates that the addition of the pyrene solution in acetone enables pyrene molecules to go into the micelle inner core. All these results showed that polymeric micelles possessing appropriate physico-chemical characteristics for drug targeting – characteristics such as diameter, CMC, and LCST – were successfully prepared from P(IPAAm-co-DMAAm)-b-PLA block copolymers.

3.3. Thermo-responsive character of the micelle inner core

We used pyrene to measure the hydrophobicity of the micelle inner core and to detect the hydrophobicity's temperature-dependent changes. The results for a polymeric micelle forming from a P(IPAAm-co-DMAAm)-b-PLA block copolymer, run 4 in Table 3, are shown in Fig. 5. In this particular field of science, researchers most frequently evaporate a pyrene-dissolving water-miscible organic solvent (e.g., acetone) in order to incorporate pyrene molecules into micelle inner cores: the process hinges on the evaporation of a water-miscible organic solvent, wherein the solvent is used to dissolve pyrene. Here, three pyrene incorporation methods were compared in terms of their possible effects on the location and the status of the incorporated pyrene molecules (e.g., pyrene molecules are distributed uniformly in the hydrophobic inner core or positioned only near the boundary between the hydrophobic inner core and the hydrophilic outer shell). In Fig. 5, the acetone method and the evaporation method yielded similar results, while the dialysis method exhibited I_1/I_3 ratios that were lower than those of the other two methods at 35 °C to 46 °C.

All three plot curves in Fig. 5 showed lower I_1/I_3 ratios at higher temperatures. This means that we did not observe a discontinuous increase in this ratio with a temperature increase around the micelles' LCST. In our preceding report [35], polymeric micelles forming from P(IPAAm)-b-poly(butyl methacrylate) block copolymers showed a significant increase in this I_1/I_3 ratio at the block copolymer's LCST. (In this case, the pyrene incorporation was made according to the acetone method.) From these facts, we concluded that

(1) the micelle inner core of the PLA did not exhibit the significant and discontinuous change in hydrophobicity that was seen in the P(IPAAm)-b-poly(butyl methacrylate) micelle system at the LCST;
(2) the dialysis method was inappropriate for correct pyrene-based detection of the inner core, possibly owing to the clustering of pyrene molecules in the inner core.

Furthermore, we examined effects that the chain length of the P(IPAAm-co-DMAAm) block had on this hydrophobicity of the inner core. We performed this examination by using three block copolymer runs (runs 4 through 6 of Table 3). These three runs were (1) almost the same in the chain lengths of the PLA blocks and (2) notably different from each other in the chain lengths of the P(IPAAm-co-DMAAm) blocks. The results are shown in Fig. 6. Micelles forming from block copolymer runs 5 and 6, which possessed longer P(IPAAm-co-DMAAm) blocks than run 4, exhibited slightly less hydrophobicity than run 4. On the other hand, all three runs were identical in that no discontinuous decrease in hydrophobicity (this is seen in the increased I_1/I_3 ratio) of the inner core corresponded to a temperature increase around the LCST. Figs. 5 and 6 reveal that the PLA micelle inner core did not show any significant change in hydrophobicity, which was observed in the P(IPAAm)-b-poly (butyl methacrylate) micelle system around the LCST.

In order to drastically change the character of the hydrophobic inner core, we used poly(ε-caprolactone) (PCL) either totally

Table 4
Syntheses of P(IPAAm-co-DAAm)-b-PCL (**5**) and P(IPAAm-co-DAAm)-b-poly(LA-co-CL) (**6**) block copolymers

Run	M.W.[1] and quantity of hydroxy-terminated P(IPAAm-co-DMAAm) (**3**) used for synthesis	ε-caprolactone	D,L-lactide	Tin(II) 2-ethyl-hexanoate	Xylene	Yield	M.W. of thermo-responsive block	M.W. of hydrophobic block[2]	M.W. and Mw/Mn of block copolymer by GPC	LCST	Unit ratio lactic acid/caprolactone
1	9000 1.08 g	0.850 g	0	21 mg	6.0 ml	51.0%	9000	2800	11,500 1.34	40.0 °C	0
2	18,600 0.839 g	0.312 g	0.850 g	46 mg	6.0 ml	59.9%	18,600	6600	27,700 2.31	38.0 °C	0.81

[1]Determined by GPC.
[2]Determined by ^{1}H NMR using M.W. of P(IPAAm-co-DMAAm).

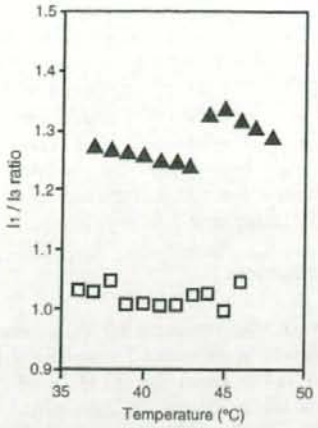

Fig. 7. Pyrene fluorescence change of polymeric micelles forming from ▲: P(IPAAm-co-DMAAm)-b-P(LA-co-CL), □: P(IPAAm-co-DMAAm)-b-PCL.

or partially for the micelle inner core. It was found that polymerization of ε-caprolactone (CL) from the terminal hydroxyl group of the P(IPAAm-co-DMAAm) chain proceeded successfully, as did copolymerization of CL with D,L-lactide. Compositions of the P(IPAAm-co-DMAAm)-b-PCL block copolymer (**5**) and of the P(IPAAm-co-DMAAm)-b-poly(LA-co-CL) block copolymer (**6**) are summarized in Table 4. Run 1 of Table 4 is the block copolymer possessing the PCL chain as the inner core-forming block. The molecular weight of its thermo-responsive P(IPAAm-co-DMAAm) block was slightly smaller (9000) than those of the P(IPAAm-co-DMAAm)-b-PLA block copolymer (**4**) runs 1 through 3 of Table 3. A molecular weight ratio between the P(IPAAm-co-DMAAm) and the hydrophobic block for this P(IPAAm-co-DMAAm)-b-PCL block copolymer (**5**) was positioned between P(IPAAm-co-DMAAm)-b-PLA runs 2 and 3 of Table 3. We observed that the polymeric micelle forming from this block copolymer **5** yielded an LCST at 40 °C. On the other hand, the unit amount of CL that belonged to the P(IPAAm-co-DMAAm)-b-poly(LA-co-CL) block copolymer (**6**, run 2 in Table 4) was larger than that unit amount of LA that belonged to the same copolymer. The LCST of this block copolymer **6** was 38 °C. Fig. 7 displays the pyrene fluorescence measurement results for the micelles that formed from these two CL-containing block copolymers. The block copolymer **5** containing the PCL block was found to possess more hydrophobic character than block copolymer **6**: the former's I_1/I_3 values were lower than the latter's. This finding was expected because the CL units were more hydrophobic than the lactic acid units. On the other hand, only micelle copolymer **6** showed, alongside a rise in temperature, a significant and discontinuous increase in the I_1/I_3 ratio. In our preceding papers [33,35], this increase was seen only for the polymeric micelles that exhibited a significant enhancement of drug release upon the temperature rise. We expected that a mechanism underlying this enhanced drug release concerned either the translocation of drugs from the hydrophobic inner core to the aggregated outer shell or water penetration into the hydrophobic inner core induced by mechanical distortion of the outer shell [47]. In Fig. 7, the increase in the I_1/I_3 ratio emerged even though the temperature showing this increase (43 °C) was considerably higher than the LCST (38 °C) determined by the optical transmittance measurements. We hypothesized that the difference in these temperatures resulted from differences in solvents used for these measurements: the fluorescence measurements were made in water, whereas the LCST determination was made in PBS. This discontinuous I_1/I_3 increase was obtained only with the P(IPAAm-co-DMAAm)-b-poly(LA-co-CL) micelle, not with either the P(IPAAm-co-DMAAm)-b-PCL micelle or the P(IPAAm-co-DMAAm)-b-PLA micelles. In general, the CL units are more hydrophobic than the lactide units, while PLA has been considered to be more rigid than PCL. In fact, we observed that the glass transition temperatures of the PLA, the PCL, and the P(LA-co-CL) block of the block copolymers were 52 °C, −47 °C, and −17 °C, respectively. These numbers indicate that the PLA block formed the glass phase inner core in a temperature range from 10 °C to 45 °C. The inner cores of the PCL and P(LA-co-CL) were in the rubber phase in this temperature range. Considering these physical properties, we expected the poly(LA-co-CL) inner core to show thermo-responsive change owing to a good balance of hydrophobicity, viscoelasticity, and other physical properties.

3.4. Doxorubicin release from polymeric micelle

We used an anticancer drug doxorubicin (DOX) for drug release experiments. DOX was successfully incorporated into polymeric micelles forming from block copolymers **5** and **6**. For both the cases, 6% of the feed DOX was incorporated. This

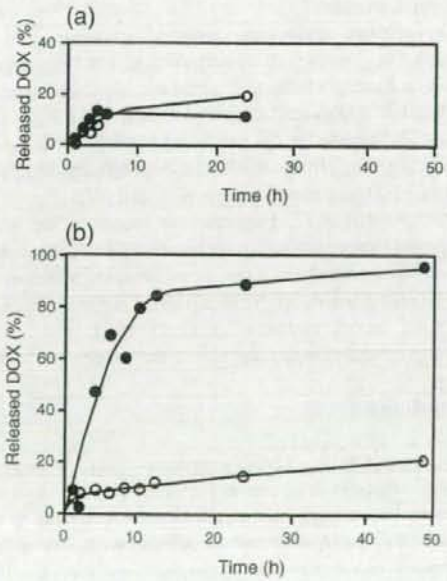

Fig. 8. Temperature-dependent drug (DOX) release from (a) P(IPAAm-co-DMAAm)-b-PCL micelle, ●: 42.5 °C and ○: 37 °C and (b)P(IPAAm-co-DMAAm)-b-P(LA-co-CL) micelle, ●: 41 °C and ○: 35 °C.

means that both of the polymeric micelles contained 15 mg of block copolymers and 0.90 mg of DOX, so long as no block copolymer loss occurred through the incorporation procedure.

To measure the release of DOX from the polymeric micelles, we used a dialysis membrane. The results of the DOX release are shown in Fig. 8. In Fig. 8(a), no enhancement of the DOX release at 42.5 °C (above the LCST) from that at 37 °C (below the LCST) was observed for the polymeric micelles of P(IPAAm-co-DMAAm)-b-PCL block copolymer **5**. In contrast, the P (IPAAm-co-DMAAm)-b-poly(LA-co-CL) (**6**) micelle provided a marked increase in the DOX release rate above its LCST in comparison with the release below the LCST, as shown in Fig. 8 (b). In our previous report [34] one composition of the P (IPAAm-co-DMAAm)-b-PLA micelles showed a significant increase (approx. five-fold) in the DOX release at 42.5 °C in comparison with the release at 37 °C. However, a big difference between the two cases emerges in relation to the absolute drug release rates. The drug release from the block copolymer micelle **6** was much more rapid than that of the P(IPAAm-co-DMAAm)-b-PLA micelle in our previous report; the former micelle released 80% of the incorporated DOX in 10 h at 41 °C, while the latter micelle showed only 15% DOX in 84 h at 42.5 °C. In the present study, no increase in the DOX release rate at the elevated temperature was observed for P(IPAAm-co-DMAAm)-b-PLA micelles (data not shown). There were differences in molecular weights of P(IPAAm-co-DMAAm)-b-PLA block copolymers between the present study and the previous one that showed a marked drug release at the elevated temperature; the molecular weights were in a range from 16,100 to 33,000 in the present study, while the molecular weight was 9300 in the previous study. Even though the cause for this difference is unknown, the polymers' molecular weight seems to impact on the thermo-responsive release.

The present study has designed an inner core-forming hydrophobic polymer chain and, in going so, has successfully detailed a biodegradable polymeric micelle drug carrier system that exhibits rapid and temperature-selective drug release behaviors. We reported in our preceding paper [35] that a polymeric micelle forming from P(IPAAm)-b-poly(butyl methacrylate) exhibited a similar thermo-responsive and quick drug release of the incorporated DOX. However, the success of the responsive and quick release is much more meaningful in the present paper because the desirable drug release control was achieved in more useful biodegradable polymeric carrier systems even though choice of biodegradable monomer units is very limited in comparison with non-biodegradable vinyl monomer units.

4. Conclusions

For this study, thermo-responsive and biodegradable polymeric micelle drug carrier systems by using a hydrophobic polyester block for the micelle inner core and a thermo-responsive poly(*N*-isopropylacrylamide-co-*N*,*N*-dimethylacrylamide) block for the outer shell of the micelle were designed and obtained. By changing the molecular weights of the two polymer blocks, we adequately controlled the micelle diameters and the critical micelle concentrations for drug targeting. At the same time, we found the phase-transition temperatures of the micelles to be determined only by the copolymer ratio of the *N*-isopropylacrylamide unit and the hydrophilic *N*,*N*-dimethylacrylamide unit. To obtain a preferred drug release behavior in terms of both substantial release rates and high thermo-responses, we oversaw the successful copolymerization of D,L-lactide and ε-caprolactone for the hydrophobic inner core-forming block.

Acknowledgement

This work was supported by the Ministry of Education, Culture, Sports, Science and Technology, Japan (a Millenium project No. 12415, Grant No. 10145104 on Priority areas, No. 296, Bio-molecular Design for Biotargeting, and the Program for Promoting the Establishment of Strategic Research Centers, Special Coordination Funds for Promoting Science and Technology), the Japan Society for the Promotion of Science (The Grant-in-Aid for Young Scientists (B) No. 16700368), and the Ministry of Health, Labour and Welfare of Japan.

References

[1] M. Page (Ed.), Tumor Targeting in Cancer Therapy, Humana Press Inc., Totowa, 2002.
[2] D.M. Brown (Ed.), Drug Delivery Systems in Cancer Therapy, Humana Press Inc., Totowa, 2004.
[3] P.A. Trail, D. Willner, S.J. Lasch, A.J. Henderson, S. Hofstead, A.M. Casazza, R.A. Firestone, I. Hellstrom, K.E. Hellstrom, Cure of xenografted human carcinomas by BR96–doxorubicin immmunoconjugates, Science 261 (1993) 212–215.
[4] L.M. Hinman, P.R. Hamann, A.T. Menendez, R. Wallace, F.E. Durr, J. Upeslacis, Preparation and characterization of monoclonal antibody conjugates of the calicheamicins: a novel and potent family of antitumor antibiotics, Cancer Res. 53 (1993) 3336–3342.
[5] P.R. Hamann, M.S. Berger, in: M. Page (Ed.), Tumor Targeting in Cancer Therapy, Humana Press Inc., Totowa, 2002, pp. 239–254.
[6] M. Singh, in: M. Page (Ed.), Tumor Targeting in Cancer Therapy, Humana Press Inc., Totowa, 2002, pp. 151–164.
[7] T. Kakudo, S. Chaki, S. Futaki, I. Nakase, K. Akaji, T. Kawakami, K. Maruyama, H. Kamiya, H. Harashima, Transferrin-modified liposomes equipped with a pH-sensitive fusogenic peptide: an artificial viral-like delivery system, Biochemistry 43 (2004) 5618–5628.
[8] D. Putnam, J. Kopecek, Polymer conjugates with anticancer activity, Adv. Polym. Sci. 122 (1995) 55–123.
[9] R. Duncan, S. Dimitrijevic, E.G. Evagorou, The role of polymer conjugates in the diagnosis and treatment of cancer, S.T.P. Pharm. Sci. 6 (1996) 237–263.
[10] A. Malugin, P. Kopeková, J. Kopecek, HPMA copolymer-bound doxorubicin induces apoptosis in human ovarian carcinoma cells by a Fas-independent pathway, Mol. Pharm. 1 (2004) 174–182.
[11] Y. Ohya, H. Oue, K. Nagatomi, K. Ouchi, Design of macromolecular prodrug of cisplatin using dextran with branched galactose units as targeting moieties to hepatoma cells, Biomacromolecules 2 (2001) 927–933.
[12] Y. Mizushima, Y. Shiokawa, M. Homma, S. Kashiwazaki, Y. Ichikawa, H. Hashimoto, A. Sakuma, A multicenter double blind controlled study of lipo-PGE1, PGE1 incorporated in lipid microspheres, in peripheral vascular disease secondary to connective tissue disorders, J. Rheumatol. 14 (1987) 97–101.
[13] S.E. Tabibi, in: D.M. Brown (Ed.), Drug Delivery Systems in Cancer Therapy, Humana Press Inc., Totowa, 2004, pp. 175–187.
[14] J. Kreuter, in: J. Kreuter (Ed.), Colloidal Drug Delivery Systems, Marcel Dekker, New York, 1994, pp. 219–342.
[15] S.M. Moghimi, C.J.H. Porter, I.S. Muir, L. Illum, S.S. Davis, Non-phagocytic uptake of intravenously injected microspheres in rat spleen:

influence of particle size and hydrophilic coating, Biochem. Biophys. Res. Commun. 177 (1991) 861–866.
[16] O. Ishida, K. Maruyama, K. Sasaki, M. Iwatsuru, Size-dependent extravasation and interstitial localization of polyethyleneglycol liposomes in solid tumor-bearing mice, Int. J. Pharm. 190 (1999) 49–56.
[17] P.G. Tardi, N.L. Boman, P.R. Cullis, Liposomal doxorubicin, J. Drug Target. 4 (1996) 129–140.
[18] M. Yokoyama, in: N. Yui (Ed.), Supramolecular Design for Biological Applications, CRC Press, Boca Raton, 2002, pp. 245–267.
[19] M. Yokoyama, in: S. Svenson (Ed.), ACS Symposium Series, Polymeric Drug Delivery I: Particulate Drug Carriers, vol. 923, American Chemical Society, 2006, pp. 27–39.
[20] A. Lavasanifar, J. Samuel, G.S. Kwon, Poly(ethylene oxide)-block-poly(L-amino acid) micelles for drug delivery, Adv. Drug Deliv. Rev. 54 (2002) 169–190.
[21] G.S. Kwon, T. Okano, Soluble self-assembled block copolymers for drug delivery, Pharm. Res. 16 (1999) 597–600.
[22] A. Marin, H. Sun, G. Husseini, W.G. Pitt, D.A. Christensen, N.Y. Rapoport, Drug delivery in pluronic micelles: effect of high-frequency ultrasound on drug release from micelles and intracellular uptake, J. Control. Release 84 (2002) 39–47.
[23] C. Allen, J. Han, Y. Yu, D. Maysinger, A. Eisenberg, Polycaprolactone-b-poly(ethylene oxide) copolymer micelles as a delivery vehicle for dihydrotestosterone, J. Control. Release 63 (2000) 275–286.
[24] D. Le Garrec, J. Taillefer, J.E. van Lier, V. Lenaerts, J.C. Leroux, Optimizing pH-responsive polymeric micelles for drug delivery in a cancer photodynamic therapy model, J. Drug Target. 10 (2002) 429–437.
[25] A. Rolland, J. O'mullane, P. Goddard, L. Brookman, K. Petrak, New macromolecular carriers for drugs. I. Preparation and characterization of poly(oxyethylene-b-isoprene-b-oxyethylene) block copolymer aggregates, J. Appl. Polym. Sci. 44 (1992) 1195–1203.
[26] M.F. Francis, M. Cristea, Y. Yang, F.M. Winnik, Engineering polysaccharide-based polymeric micelles to enhance permeability of Cyclosporin A across Caco-2 cells, Pharm. Res. 22 (2005) 209–219.
[27] K. Maruyama, S. Unezaki, N. Takahashi, M. Iwatsuru, Enhanced delivery of doxorubicin to tumor by long-circulating thermosensitive liposomes and local hyperthermia, Biochim. Biophys. Acta 1149 (1993) 209–216.
[28] J.N. Weinstein, R.L. Magin, M.B. Yatvin, D.S. Zaharko, Liposomes and local hyperthermia: selective delivery of methotrexate to heated tumors, Science 204 (1979) 188–191.
[29] M. Yokoyama, in R. Arshady (Ed.), The MML Series—Microspheres, Microcapsules and Liposomes, vol. 7, Citus Books, London (in press).
[30] J.E. Chung, M. Yokoyama, K. Suzuki, T. Aoyagi, Y. Sakurai, T. Okano, Reversibly thermo-responsive alkyl-terminated poly(N-isopropylacrylamide) core-shell micellar structures, Colloids Surf., B Biointerfaces 9 (1997) 37–48.
[31] J.E. Chung, M. Yokoyama, T. Aoyagi, Y. Sakurai, T. Okano, Effect of molecular architecture of hydrophobically modified poly(N-isopropylacrylamide) on the formation of thermoresponsive core-shell micellar drug carriers, J. Control. Release 53 (1998) 119–130.
[32] F. Kohori, K. Sakai, T. Aoyagi, M. Yokoyama, Y. Sakurai, T. Okano, Preparation and characterization of thermally responsive block copolymer micelles comprising poly(N-isopropylacrylamide-b-DL-lactide), J. Control. Release 55 (1998) 87–98.
[33] J.E. Chung, M. Yokoyama, M. Yamato, T. Aoyagi, Y. Sakurai, T. Okano, Thermo-responsive drug delivery from polymeric micelles constructed using block copolymers of poly(N-isopropylacrylamide) and poly(butylmethacrylate), J. Control. Release 62 (1999) 115–127.
[34] F. Kohori, K. Sakai, T. Aoyagi, M. Yokoyama, M. Yamato, Y. Sakurai, T. Okano, Control of adriamycin cytotoxic activity using thermally responsive polymeric micelles composed of poly(N-isopropylacrylamide-co-N, N-dimethylacrylamide)-b-poly(DL-lactide), Colloids Surf., B Biointerfaces 16 (1999) 195–205.
[35] J.E. Chung, M. Yokoyama, T. Okano, Inner core segment design for drug delivery control of thermo-responsive polymeric micelles, J. Control. Release 65 (2000) 93–103.
[36] F. Kohori, M. Yokoyama, K. Sakai, T. Okano, Process design for efficient and controlled drug incorporation into polymeric micelle carrier systems, J. Control. Release 78 (2002) 155–163.
[37] I.M. Hamse, M.D.C. Topp, P.J. Dijkstra, J. Feijen, Entrapment of hydrophobic molecules in PEG-PNIPAAm block copolymers, J. Control. Release 64 (2000) 273–274.
[38] M.D.C. Topp, P.J. Dijkstra, H. Tapsma, J. Feijen, Thermosensitive micelle-forming block copolymers of poly(ethylene glycol) and poly(N-isopropylacrylamide), Macromolecules 30 (1997) 359–373.
[39] D. Neradovic, C.F. van Nostrum, W.E. Hennink, Thermosensitive degradable polymeric micelles for controlled drug delivery, Proceedings of the 28th International Symposium on Controlled Release of Bioactive Materials, 2001, #5060.
[40] M. Yokoyama, A. Satoh, Y. Sakurai, T. Okano, Y. Matsumura, T. Kakizoe, K. Kataoka, Incorporation of water-insoluble anticancer drug into polymeric micelles and control of their particle size, J. Control. Release 55 (1998) 219–229.
[41] M. Yokoyama, P. Opanasopit, Y. Maitani, K. Kawano, T. Okano, Polymer design and incorporation method for polymeric micelle carrier system containing water-insoluble anti-cancer agent camptothecin, J. Drug Target. 12 (2004) 373–384.
[42] R. Yoshida, K. Uchida, Y. Kaneko, K. Sakai, A. Kikuchi, Y. Sakurai, T. Okano, Comb-type grafted hydrogels with rapid deswelling response to temperature changes, Nature 374 (1995) 240–242.
[43] Y. Kaneko, K. Sakai, A. Kikuchi, R. Yoshida, Y. Sakurai, T. Okano, Influence of freely mobile grafted chain length on dynamic properties of comb-Type grafted poly(N-isopropylacrylamide) hydrogels, Macromolecules 28 (1995) 7717–7723.
[44] M. Matsukata, T. Aoki, K. Sanui, N. Ogata, A. Kikuchi, Y. Sakurai, T. Okano, Effect of molecular architecture of poly(N-isopropylacrylamide)–Trypsin conjugates on their solution and enzymatic properties, Bioconjug. Chem. 7 (1996) 96–101.
[45] L.W. Seymour, R. Duncan, J. Strohalm, J. Kopecek, Effect of molecular weight (Mw) of N-(2-hydroxypropyl)methacrylamide copolymers on body weight distribution and rate of excretion after subcutaneous, intraperitoneal, and intravenous administration to rats, J. Biomed. Mater. Res. 21 (1987) 1341–1358.
[46] T. Cao, P. Munk, C. Ramireddy, Z. Tuzar, S.E. Webber, Fluorescence studies of amphiphilic poly(methacrylic acid)-block-polystyrene-block-poly(methacrylic acid) micelles, Macromolecules 24 (1991) 6300–6305.
[47] M. Yokoyama, in: N. Yui (Ed.), Supramolecular Design for Biological Applications, CRC Press, Boca Raton, 2002, pp. 245–267.

Chapter 3

Polymeric Micelle Drug Carriers for Tumor Targeting

Masayuki Yokoyama

Kanagawa Academy of Science and Technology, KSP East 404, Sakado 3–2–1, Takatsu-ku, Kawasaki-shi, Kanagawa-ken 213–0012, Japan (email: masajun@ksp.or.jp)

The methodology of targeting of anti-cancer drugs to solid tumors using polymeric micelle drug carriers is described. Polymeric micelles inherently possess several strong advantages owing to their physico-chemical properties for tumor targeting by a passive targeting mechanism called Enhanced Permeability and Retention (EPR) effect. Several examples for the tumor targeting are discussed.

Introduction

Targeting of Anti-cancer Drugs to Solid Tumors

Drug targeting is defined as selective drug delivery to specific sites, organs, tissues or cells, where drug activities are required. By increasing delivery to the therapeutic sites and reducing delivery to unwanted sites, an improved therapeutic index can be obtained with enhanced drug action at the therapeutic site. Drug targeting can be classified into two methods: active and passive targeting (*1,2*). Active targeting aims at an increase in the delivery of drugs to the target by utilizing biologically specific interactions such as antigen–antibody binding or by utilizing locally applied signals such as heating and sonication. Carriers classified in this method include specific antibodies, transferrin, and thermo-responsive liposomes and polymeric micelles. Passive targeting is defined as a method whereby the physical and chemical properties of carrier systems increase the target/non-target ratio of a quantity of a delivered drug. Which method, active or passive targeting, is superior and more applicable to tumor targeting? Both methods are important for drug targeting, however, it should be emphasized that factors governing passive targeting are also important for active targeting systems for the following reasons:

(1) The vast majority of a living body comprises non-target sites. Even the liver, one of the largest targets of drugs, only occupies approximately 2% of the weight of the entire body. That is, 98% of the body can be considered to be non-target sites, while active targeting can only be achieved within the remaining small body fraction. Minimizing non-specific capture at non-target sites by passive targeting may therefore be important to maximize the amount delivered to active targeting sites.

(2) Passive targeting precedes active targeting in most cases. Exceptions are cases for intravascular targets such as lymphocytes and vascular endothelial cells. Most targets are located in the extravascular space. To reach these targets via the bloodstream, the first step must be extravasation through the vascular endothelia, followed by permeation through the interstitial space to the extravascular targets.

Targeting of anti-cancer drugs to solid tumors using polymeric micelles has been studied mostly with respect to passive targeting, and therefore, only passive targeting to solid tumors is discussed in this chapter.

Passive targeting of polymeric micelles to solid tumors can be achieved through the Enhanced Permeability and Retention (EPR) effect, presented by Maeda and Matsumura in 1986 (*3,4*). As illustrated in Figure 1, the vascular permeability of tumor tissues is enhanced by secreted factors such as kinin. As a result of this increased vascular permeability, macromolecules increase their transport from blood vessels to tumor tissues, while small molecules do not change their transport. Furthermore, the lymphatic drainage system does not operate effectively in tumor tissues, and therefore, macromolecules are selectively retained for a prolonged time period in the tumor interstitium. For utilizing the EPR effect, specific targeting moieties such as antibodies are not necessary. As a result of this effect, macromolecules including polymeric micelles can selectively accumulate at solid tumor sites.

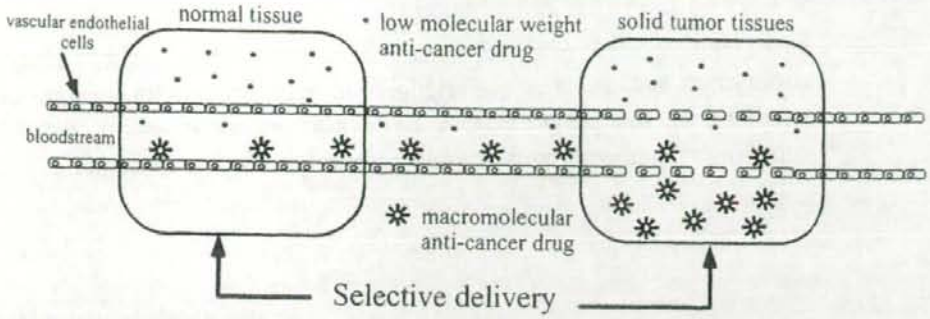

Figure 1. Enhanced Permeability and Retention (EPR) effect of macromolecules at solid tumor tissues.

However, carrier polymers must fulfill two requirements to avoid non-specific capture at non-tumor sites:

(1) Drug carriers must possess an appropriate size or molecular weight. The diameter of a carrier must be smaller than ca. 200 nm if the reticuloendothelial system's uptake is to be evaded (*5*). Additionally, molecular weights larger than the critical value of approximately 40,000 Da are favorable for evading renal filtration.

(2) Drug carriers must not strongly interact or even being taken up by normal organs, especially the reticuloendothelial systems. This behavior is typically observed for cationic and hydrophobic polymers (*6*). Therefore, carrier polymers should be hydrophilic with neutral or weak negative overall charge, and they should not contain chemical structur elements that would be biologically recognizable to normal tissues.

Because polymeric micelles are formed in a diameter range from 10 to 100 nm, the size requirement for the EPR effect is inherently fulfilled. Furthermore, the charge requirement can be easily fulfilled by the use of hydrophilic and neutral or weakly negative-charged polymers as building block for the outer shell.

Results and Discussion

Advantages of Polymeric Micelles for TumorTargeting

A polymeric micelle is a macromolecular assembly that forms from block or graft copolymers, has a spherical inner core and an outer shell (*7*). As shown in Figure 2 in which an AB-type block copolymer is being used, a micellar structure forms if one segment of the block copolymer can provide enough interchain cohesive interactions in a solvent. Most studies of polymeric micelles, both in

basic and applied research, have been done with AB or ABA-type block copolymers because the close relationship between micelle-forming behavior and structure of the polymers can be evaluated more easily with these block copolymers than with graft or multi-segmented block copolymers.

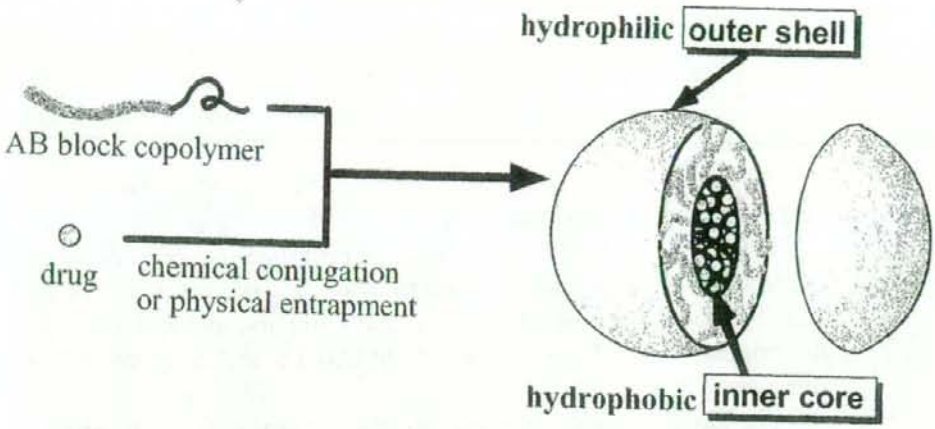

Figure 2. Formation of polymeric micelles as drug carriers.

The cohesive interactions in the inner core utilized as the driving force for micelle formation include hydrophobic, electrostatic, and π–π interactions as well as hydrogen bonding. Because most anti-cancer drug molecules possess a hydrophobic character, hydrophobic interactions are most commonly used for tumor targeting (*8-20*). Drugs can be incorporated into polymeric micelles both by chemical conjugation and physical entrapment. Polymeric micelles possess strong and unique advantages for tumor targeting, which are summarized in Table I.

Table I. Advantages of polymeric micelles for tumor targeting

Very small diameter (10 – 100 nm)
High structural stability
High water solubility
Low toxicity
Separated functionality

First, polymeric micelles are formed typically in a diameter range from 10 to 100 nm, with very narrow size distribution. This size range is considered ideal for the attainment of tumor targeting by the EPR effect because it evades the

reticuloendothelial system's uptake and renal excretion. Second, polymeric micelles possess high structural stability, provided by the entanglement of polymer chains in the inner core. This stability has static and dynamic aspects (*21-24*). Static stability is described by a critical micelle concentration (cmc). Generally, polymeric micelles show very low cmc values in a range form 1 to 10 μg/mL. These values are much smaller than typical cmc values of micelles forming from low molecular weight surfactants. The dynamic stability is described by low dissociation rates of micelles, and this aspect might be more important for in-vivo drug delivery in physiological environments, which are in non-equilibrium conditions. The high structural stability of polymeric micelles is an important key to drug delivery through micelles and eliminates the possible contribution of single polymer chains as drug carriers. The third advantage is the high water solubility of polymeric micelles encapsulating hydrophobic anti-cancer drugs. In conventional polymeric drug carrier systems, a loss of water solubility of the polymeric carrier resulting from the interaction with a hydrophobic drug creates a serious problem. Drug conjugation to a homo-polymer easily leads to precipitation because of the high, localized concentration of hydrophobic drug molecules bound along the polymer chain. Several research groups reported this problem during synthesis of drug–homopolymer conjugates (*25-27*) and during their intravenous injections (*28*). Therefore, conventional drug–polymer conjugates must be designed with considerably low drug content to avoid or reduce the risk of precipitation. In contrast, polymeric micelles maintain their water solubility because the hydrophilic outer shell works as a barrier against intermicellular aggregation of the hydrophobic cores. This results in much larger hydrophobic drug contents for these carriers than carriers based on conventional polymers. For example, the maximum loading of anticancer drugs adriamycin or daunomycin (an adriamycin derivative) was reported to range from 10 to 35 wt% for conventional polymer-drug conjugates (*25,26,29,30*), while a polymeric micelle system contained 60 wt% of adriamycin (*31*). This advantage is especially important in cancer chemotherapy because most of recently developed anti-cancer drugs are strongly hydrophobic.

The beneficial character of low toxicity may be described as the forth advantage. In general, polymeric surfactants are known to be less toxic than low molecular weight surfactants such as sodium dodecyl sulfate, as exemplarily shown for Pluronic (*32*). Furthermore, polymeric micelles are considered very safe with respect to chronic toxicity. Possessing a much larger size than the critical filtration values in the kidney, polymeric micelles can evade renal filtration, even if the molecular weight of the constituting block copolymer is lower than the critical molecular weight for renal filtration. In addition, all constituent polymer chains of a polymeric micelle can be released as single strands from the micelle during a long time period because these strands are not chemically bound to each other. This phenomenon results in complete excretion of the block copolymers from the renal route if the polymer chains are designed with a lower molecular weight than the critical value for the renal filtration. This phenomenon is a huge advantage of polymeric micelles over conventional (non-micelle forming) and non-biodegradable polymeric drug carriers. The fifth advantage is separated functionality. Polymeric micelles are composed of two

phases, the inner core and the outer shell. Various functions required for drug delivery systems can be shared by these structurally separated phases. For example, the outer shell is responsible for interactions with biocomponents such as proteins and cells. These interactions determine where drug carriers go in the living body; and therefore, the shell controls the in-vivo delivery of drugs. The inner core is responsible for pharmacological activities through drug loading and release. The properties of both phases are independently controlled through the selection of the respective constituent block of the polymer strand and makes this heterogeneous structure more favorable for the construction of highly functionalized carrier systems than conventional (non micelle-forming) polymeric carriers.

Examples of Anti-cancer Drug Targeting to Solid Tumors

1. Adriamycin (Doxorubicin)

Yokoyama, Kwon, Okano, and Kataoka et al. succeeded in targeting the anticancer drug adriamycin (ADR) (= doxorubicin) to solid tumors, using a polymeric micelle system (*33-36*). Adriamycin was chemically conjugated to aspartic acid residues of poly(ethylene glycol)–poly(aspartic acid) block copolymers, PEG-P(Asp) by amide bond formation. The PEG segment was hydrophilic, whereas the ADR-substituted P(Asp) chain was hydrophobic. Therefore, the obtained drug–block copolymer conjugate PEG–P(Asp)-ADR formed micellar structures owing to its amphiphilic character. On the second step, ADR was incorporated into the hydrophobic inner core by physical entrapment. As a result, polymeric micelles containing both the chemically conjugated and the physically entrapped ADR were obtained with the PEG outer shell.

As shown in Figure 3, the physically entrapped ADR was present at much higher concentrations for a long time-period (Fig. 3a) and was delivered to the solid tumor site at much higher concentrations than free ADR (Fig. 3b) (*37*). The observed time profile with a peak concentration at 24 hours post intravenous injection and an extended retention of this high concentration post injection matched well with passive delivery by the EPR effect (*3*). On the other hand, accumulation of the physically entrapped ADR at normal organs and tissues was the same or lower than observed for free ADR.

In accordance with this highly selective delivery to solid tumor sites, a dramatic enhancement of anti-tumor activity was observed (*37*). Figure 4 shows in-vivo anti-tumor activity against murine colon adenocarcinoma 26. For free ADR, only the maximum tolerated dose (10 mg/kg body weight) provided considerable inhibition effects on tumor growth; however, a decrease in tumor volume was never seen from the day of the first injection. For the polymeric micelles, the tumor completely disappeared in two doses (20 and 10 mg physically entrapped ADR/kg of body weight). These results clearly demonstrate the successful passive targeting of an anti-cancer drug using a polymeric micelle carrier system to a tumor. This adriamycin-containing system has passed a Phase I clinical trial and entered the Phase II trial in autumn of 2003 at the National Cancer Hospital in Japan.